Ultrasound and Microbubbles Combined with Gold Nanoparticles Enhanced the Therapeutic Effect of Radiotherapy in Breast Cancer Cells

Amanda Thu Lee Tran (MSc)[1]
Jean-Philippe Pignol (MD, PhD)[2]
Gregory J. Czarnota (MD, PhD)[2]
Raffi Karshafian* (PhD)[1]
1 Department of Physics, Ryerson University, 350 Victoria Street, Toronto, Canada, M5B-2K3
2 Sunnybrook Odette Cancer Centre, 2075 Bayview Avenue, Toronto, M4N-3M5 Canada

***Corresponding author:**
Raffi Karshafian
Email: karshafian@ryerson.ca
Ryerson University
350 Victoria Street, KHE 329 E
Toronto, Ontario, Canada, M5B-2K3
Tel: 1-416-979-5000 ext 7536
Fax: 1-416-979-5343

***Keywords**: Ultrasound therapy, sonoporation, gold nanoparticles, radiotherapy, radiosensitization*

Abbreviations
USMB Ultrasound and microbubbles
AuNP Gold Nanoparticles
XRT Ionizing Radiation
V_A Expected additive cell viability
V_C Measured clonogenic cell viability

Abstract

Gold nanoparticles have been shown to enhance local radiation dose due to its high Z value. Ultrasonically-stimulated microbubbles at therapeutic conditions can sensitize cells to ionizing radiation and enhance cell permeability allowing gold nanoparticles to cross the plasma membrane. In this study, ultrasound-microbubble potentiated enhancement of cell death in combination with gold nanoparticles and ionizing radiation is investigated *in vitro*. A suspension model of breast cancer (MDA-MB-231) cells was exposed to ultrasound and microbubbles (USMB), gold nanoparticles (AuNP) and ionizing radiation (XRT). A 12 nm spherical AuNPs at concentrations of 7.8 $x10^{10}$ nps/mL and 1.6 x 10^{11} nps/mL were investigated at fixed USMB conditions of 500 kHz pulse center frequency, 580 kPa peak negative pressure, 10 µs pulse duration, 60s insonation time, Definity® microbubbles at 3.3% (v/v) and XRT dose of 2 Gy. Cell viability post treatment was evaluated using clonogenic assay. The application of AuNP and USMB induced a synergistic increase in cell death when combined with XRT. A 22 fold increase in cell death was observed with the combined treatment (AuNP+USMB+XRT=3±0.4%) compared to radiotherapy only (XRT=65±3%). The combined treatment of ultrasound-

microbubbles with gold nanoparticles followed by radiotherapy induced a synergistic effect in cell death.

Introduction

Therapeutic ultrasound, guided by imaging modalities, can selectively enhance treatment of diseased tissues while sparing surrounding normal tissue by focusing the acoustic energy within the body non-invasively (1, 2). The application of therapeutic ultrasound in combination with microbubbles (USMB) has been shown to enhance radiotherapy and chemotherapy in preclinical tumour models (3-6). Microbubble agents, comprised of shell-encapsulated gas-core bubble, are generally less than 5 μm allowing them to pass through the systemic circulation following peripheral venous administration (7). The combined treatment of USMB and radiotherapy synergistically enhanced cell death, a ~10 fold increase, of prostate cancer (PC3) xenograft tumours (8, 9). In addition, the combination of USMB and chemotherapeutic agents has significantly improved therapeutic outcome of chemotherapy in cancer models (3, 10-12). Furthermore, the ability of USMB to damage the microvasculature has been demonstrated; both non-reversible anti-vascular effect and reversible shutdown of blood flow with fast flow-recovery (~few minutes) has been observed (13). More recently, it was shown that USMB enhanced the thermal dose of gold nanoparticles combined with laser therapy, inducing a synergistic enhancement in cell death (14, 15). The mechanism with USMB potentiated therapies has been shown to be associated with biomechanical perturbation of plasma membrane, generating pores of around 50-100 nm, and of blood vessels. The phenomenon of generating transient and reversible changes in cell membrane permeability is known as *sonoporation* (16-21). In addition, it has been demonstrated that the application of USMB can enhance radiation response through biomechanical perturbation of cell membranes causing ceramide production (22-24). Furthermore, USMB has been shown to induce anti-vascular effects (25-28).

The therapeutic effects of radiotherapy can be enhanced in the presence of gold nanoparticles (AuNP); it has been shown that cell death increases by up to 3 fold (29, 30). AuNPs have been investigated as a method to radiosensitize cancerous cells due to a high atomic number and their relatively inert nature. Upon irradiation of gold atoms with low energy photons, the photoelectric effect dominates ejecting inner atomic shell electrons. The atomic shell reorganizes, known as an Auger cascade, and emits a localized dose of radiation at microscopic scale (31). These characteristics make AuNPs a viable radiosensitizing agent in radiotherapy (32, 33). The delivery of AuNPs to cancerous tissues can be achieved through a passive preferential uptake, known as enhanced permeability and retention (EPR) effect (34). The EPR effect has been shown to improve *in vivo* tumour response when followed by radiotherapy (35, 36). AuNP can cross the plasma membrane through endocytosis (37, 38), however, delivery efficiency depends on the AuNP size, shape and concentration (39, 40). The uptake of AuNP can be enhanced by coating AuNPs with biological targeting molecules (41, 42), and more recently through the application of USMB (14, 15). In this work, the effect of USMB in combination with AuNP and XRT in killing cancer cells is investigated in a breast cancer cell line. Cells in suspension were treated with AuNPs, USMB, XRT and their combinations at varying AuNP concentrations. Following the treatment, cell viability was assessed using clonogenic assay.

Materials and Methods

In vitro cell model

A human adenocarcinoma breast cell line (MDA-MB-231) from the American Type Culture Collections (ATCC, MD, USA) was cultured in RPMI-1640 medium supplemented with 5% penicillin/streptomycin antibiotic and 10% fetal bovine serum. The cells were incubated at 37°C and 5% CO_2 concentration. Cells were washed with Dulbecco's Phosphate Buffered Saline (DPBS), trypsinized and suspended in media at a concentration of $1.5x10^6$ cells/mL.

Gold nanoparticles (AuNP)

Gold nanoparticle spheres (AuNP) of 12±1.5 nm in size prepared at $5.1x10^{11}$ nps/mL in Milli-Q water (no CTAB content) were added to the cell suspension (Nanopartz™, Inc., Loveland, CO, USA). The concentrations of AuNP used were $7.8x10^{10}$ nps/mL and $1.6x10^{11}$nps/mL corresponding to 60 nM and 116 nM for AuNP, respectively. Cells were incubated with AuNP for 5 minutes at room temperature and treated with XRT within 10 minutes without and with centrifuging the samples prior to XRT. The centrifuging process removes the AuNP from the cell suspension.

Ultrasound and microbubble treatment

Cells were exposed to ultrasound in the presence of Definity® (Lantheus Medical Imaging, Inc., North Billerica, MA, USA) microbubbles, which is a clinically approved ultrasound contrast agent. The ultrasound exposure system consisted of a single element transducer of 500 kHz center-frequency with 28.6 mm element diameter focused at 85 mm and a – 6dB beam width of 31 mm at the focal point (IL0509HP; Valpey Fisher Inc, Hopkinton, MA, USA). The transducer was mounted to a micro-positioning system, and connected to a power amplifier (RPR4000, Ritec Inc., Warwick, RI) and a waveform generator (AWG520, Tektronix Inc., Beaverton, OR). The cell exposure chamber was of cylindrical shape with 12 mm internal diameter and 10 mm diameter with Mylar membrane windows across the cylinder and a magnetic stirrer within the chamber (Figure 1).

A 3 mL volume of cells in suspension was placed in the exposure chamber along with AuNP and microbubbles and then exposed to ultrasound pulses at 32 μs pulse duration, 1 kHz pulse repetition frequency, and 60 s insonation time at 580 kPa negative peak pressure in the presence of 3.3% v/v (volume concentration) of Definity microbubbles. The USMB exposure conditions used in this study were based on our previous published studies optimizing intracellular uptake of cell-impermeable molecules (16, 17). Following USMB and AuNP+USMB exposure, cells were treated with XRT within 10 minutes without and with centrifuging the samples, which removes the AuNP from the cell suspension prior to XRT.

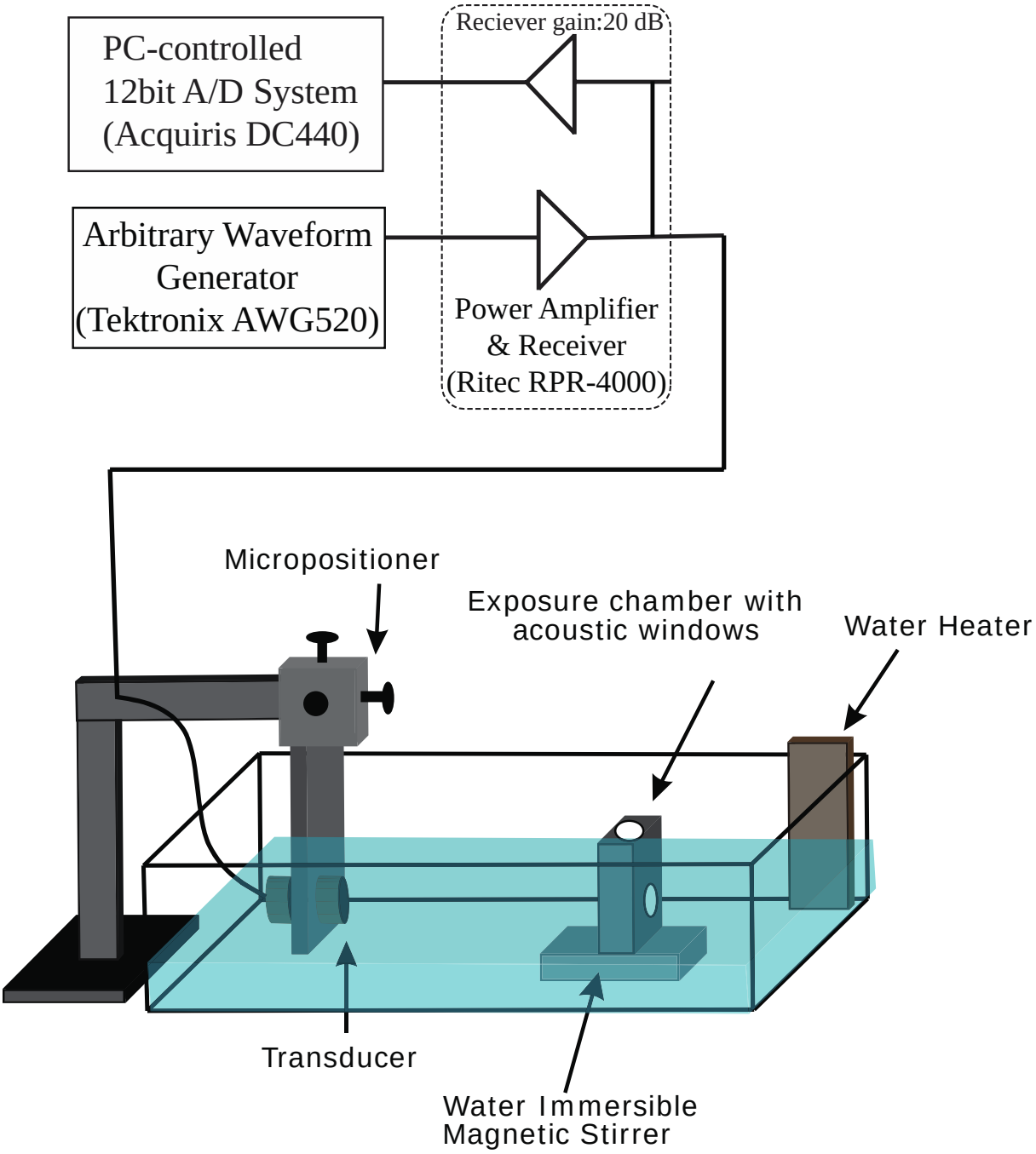

Figure 1: A schematic diagram of the ultrasound exposure apparatus of the cell suspension system.

Ionizing Radiation (XRT)

Prior to XRT treatment, cells were transferred to 35 mm Petri dishes and irradiated with 2 Gy single fraction dose at 160 kVp and 200 cGy/min dose rate (Faxitron Xray Corporation, Lincolnshire, IL, USA). Cells were exposed to XRT with and without AuNP in the solution of the cell suspension. XRT treatment was performed either following centrifugation of cell-AuNP suspension to remove excess AuNP from solution (that is, XRT without AuNP in solution) or without centrifuging where cells were exposed to XRT with AuNP in suspsension (that is, XRT with AuNP in solution of the cell suspension).

Clonogenic assay

Following the combined treatment of AuNP, USMB and XRT, cell viability was assessed using clonogenic assay (V_C). Cells were plated in 50 mm culture dishes and incubated for 13-15 days. The cells were then stained with methylene blue and clusters of more than 50 cells counted. Experiments were repeated with four independent samples, and colony assay was done in triplicate (n=12).

Analysis

Synergism of the combined treatment was assessed using the Bliss independence criterion (43), where the expected additive effect on cell viability (V_A) for the combined therapy was compared to experimental measurements. The expected additive response of the combined treatments was calculated based on the measured cell viability (V_C) of each treatment. The combined treatment was considered synergistic when V_C was statistically lower than V_A. A Tukey post-hoc was done to compare each treatment and determine its significance. V_A and V_C were compared using a non-parametric t-test.

Results

AuNP Spheres with USMB and XRT

Clonogenic viability of cells treated with USMB, XRT and AuNP spheres (12 nm) is shown in Figure 2; (A) and (B) represents samples without AuNP in the suspending solution (centrifuged samples) and with AuNP in the suspending solution (non-centrifuged samples), respectively. Cell viability decreased by 22 and 11 folds with AuNP+USMB+XRT compared to XRT alone and AuNP+XRT, respectively. A statistically lower cell-viability was achieved with the combined treatment of AuNP+USMB+XRT (V_C=3±0.4%) compared to XRT alone (V_C=65±3%) and to AuNP+XRT (V_C=34 ±1%) (Fig.2A). Cell viability with AuNP and USMB or XRT appeared to be independent of AuNP concentration. Viability with AuNP+USMB was 37±4% and 41±4%, and with AuNP+XRT was 34±2% and 34±1% at low and high spherical AuNP concentrations, respectively. Whereas, in the combined treatment of AuNP+USMB+XRT, a statistically lower cell-viability was achieved at the higher spherical AuNP concentration (V_C=3±0.4%) compared to the lower AuNP concentration (V_C=14 ±2%). In addition, a statistically lower cell-viability was achieved with USMB+XRT (V_C=18±2%) compared to XRT alone (V_C=65±3%) and USMB alone (V_C=58±4%). No statistically significant difference was observed with AuNP alone compared to untreated control, whereas, viability of cells treated with AuNP+USMB decreased by 20% compared to USMB alone. Furthermore, the presence of spherical AuNP in the cell suspension (without centrifuging the sample prior to XRT) in AuNP+XRT treatment (V_C~25%) decreased cell viability by 2 fold compared to centrifuged AuNP+XRT (Fig.2B). A

similar fold decrease in cell viability was observed in AuNP+USMB+XRT with the presence AuNP in the solution.

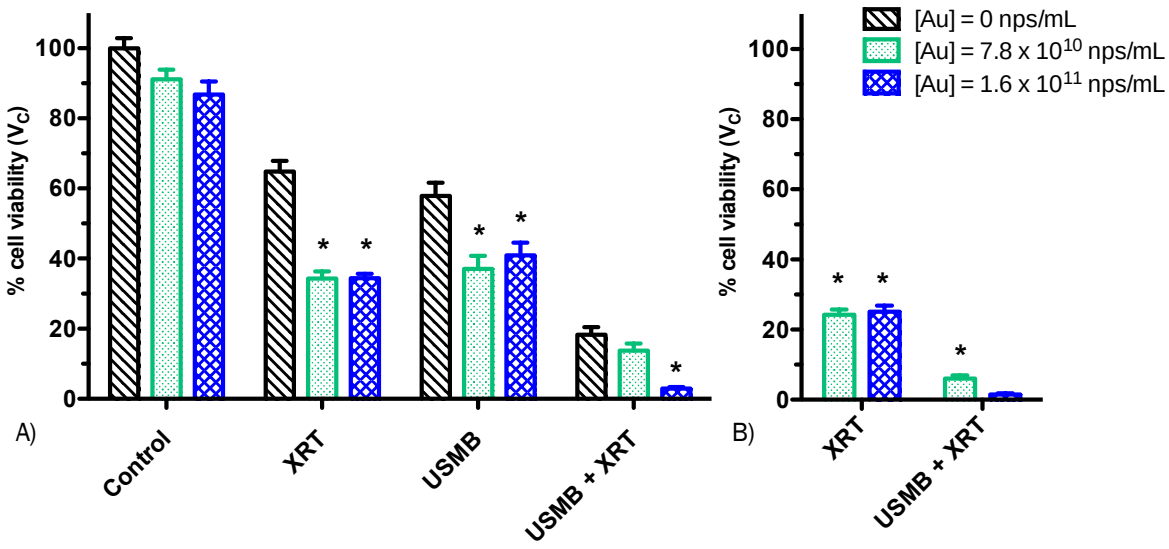

Figure 2: Clonogenic viability of MDA-MB231 cells exposed to 12 nm AuNP spheres normalized with control. a) Two different concentrations of AuNP, USMB fixed at 0.5 MHz frequency pulses with 580 kPa negative peak pressure and 3.3% (v/v) microbubbles, and a 160 kVp 2Gy single radiation dose and their combinations are shown. The asterisks signify its statistical significance ($p < 0.01$) in comparison to samples without AuNPs, 0 nps/mL concentration. The cell viability of AuNP, USMB, and XRT combined treatments with b) gold within solution. The asterisks in Figure 1b) represents its statistical significance compared with its counter condition in Figure 1a). The error bars represent the standard error of the mean.

Synergism of combined treatments

The calculated additive effect of the combined treatments on cell viability (V_A) with different permutations of AuNP, USMB and XRT using the Bliss independence criterion for spherical AuNP is shown in Figure 3. The combined USMB+XRT treatment induced a synergistic effect on cell viability (that is, V_C was statistically less than V_A), as expected, whereas the combined treatment was additive with AuNP+USMB (Fig.3A). In addition, a synergistic effect on cell viability was induced with AuNP+USMB+XRT at all conditions compared to the additive effect of three treatments: AuNP, USMB and XRT. A V_C of 3±0.4% (AuNP at $1.6x10^{11}$ nps/mL) compared to V_A of 33±3% based on the experimental cell viability observed with each of the single treatments (V_C of 87±4%, 58±4% and 65±3% with AuNP, USMB and XRT, respectively). Furthermore, AuNP in all permutations achieved a synergistic effect at AuNP concentrations of 1.6×10^{11} nps/mL, however showed no synergistic effect with AuNP concentrations of 7.8×10^{10} nps/mL with a V_C of 13% and V_A of 34% (Fig.3B). Whereas, synergism was

achieved with the additive combination of (AuNR+XRT) with USMB and (AuNR+USMB) with XRT.

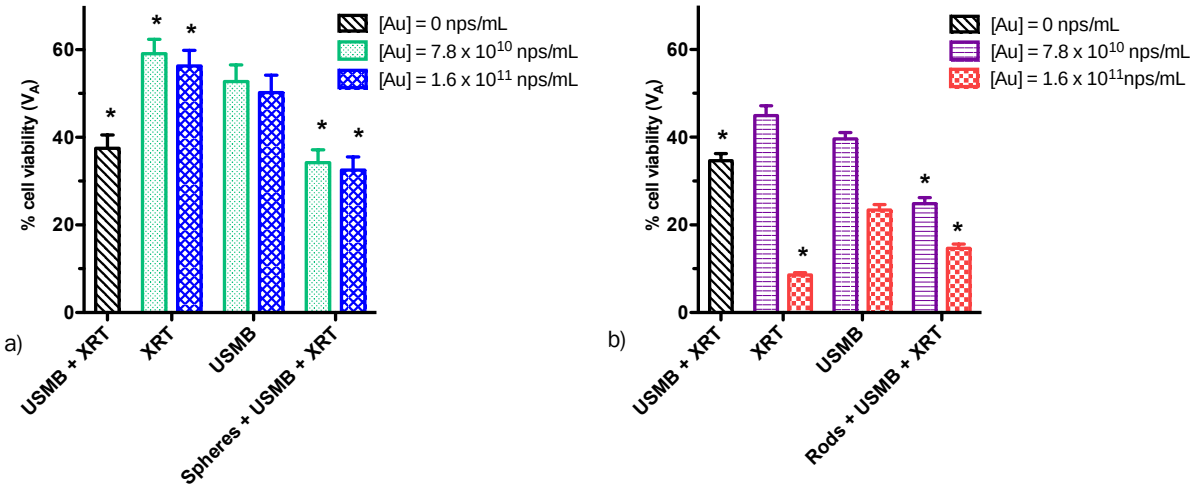

Figure 3: The calculated additive effect (V_A) of AuNP, USMB, and XRT on a) AuNP and b) AuNR. The asterisks identify the treatments that have a statistically significant $V_C > V_A$. The error bars represent the standard error of the mean.

Discussion

This study demonstrated for the first time a significant radiosensitization effect of ultrasound and microbubbles with gold nanoparticles and ionizing radiation. Cell viability decreased by up to 22 fold using spherically shaped AuNP of 12nm diameter at a concentration of 116 nM and a clinically relevant dose of 2 Gy. It has been shown that in addition to the gold nanoparticle size, the microscopic localization of the AuNP plays also an important role (44). This is especially true for low energy sources like 160 kVp beams as used in this study. AuNP can be manufactured at various sizes and shapes, and conjugated with biological molecules to maximize delivery to biological tissues including cells, however, the hydrophobic nature of the semi-permeable lipid bilayer of a cell membrane prevents large molecules to diffuse across. Many studies have shown that AuNP accumulation *in vitro* is primarily due to endocytosis and depends on AuNP size and shape, and surface characteristics (37, 38, 40). Coated AuNP with bifunctional-PEG under 40 nm in size have been shown to improve circulation time (45) and prevent *in vivo* renal retention (46) resulting in enhanced tumour uptake. For therapeutic effect, an incubation time of 16 hours – 15 days of PEG-AuNP may be necessary prior to irradiation (45, 47). In addition, the clinical applications of gold nanoparticles remain limited by the amount of AuNP that can be administered to the patient and their localization in the vicinity or inside cancer cells (38, 48, 49). Our results suggest that the application of ultrasound-and-microbubbles can potentially address these limitations by reducing the dose of gold nanoparticles and improve local delivery. Furthermore, the enhanced therapeutic effect of the combination of USMB with ionizing

radiation further makes this strategy clinically appealing.

The mechanism of synergistic enhancement of cell death with the combined treatment of AuNP, USMB and XRT is associated with ultrasound and microbubble induced uptake of gold nanoparticles and biomechanical perturbation of cell membranes (50-52) causing an increase in ceramide production, which in turn can induce apoptosis (23). Ultrasonically-stimulated microbubbles generates transient pores within the cell membrane allowing AuNP to enter the cell, which results in an increased radiosensitization. The enhanced uptake of AuNP and radiosensitivity by ultrasound-microbubble indicates a possible mechanism for the synergistic effect of AuNP, USMB and XRT and its dependence on concentration in an *in vitro* setting.

Conclusions

The combined treatment of gold nanoparticles, ultrasound-microbubbles, and ionizing radiation is synergistic in MDA-MB-231 cells compared to nanoparticles and ionizing radiation. Cell viability decreased by 22 fold with the combined treatment compared to XRT alone. The synergistic effects depended on the concentration and the location of AuNP. This study demonstrates that the combined treatment of AuNP+USMB+XRT may significantly enhance the desired effect of radiotherapy and decrease the amount of AuNP required for a therapeutic effect.

Acknowledgments

The research was supported by grants from The Terry Fox Foundation and NSERC Discovery.

References

[1] Goertz DE. An overview of the influence of therapeutic ultrasound exposures on the vasculature: High intensity ultrasound and microbubble-mediated bioeffects. International Journal of Hyperthermia. 2015; 31(2):134-44.
[2] Unger EC, Porter T, Culp W, et al. Therapeutic applications of lipid-coated microbubbles. Adv Drug Deliv Rev. 2004; 56(9):1291-314.
[3] Goertz DE, Todorova M, Mortazavi O, et al. Antitumor Effects of Combining Docetaxel (Taxotere) with the Antivascular Action of Ultrasound Stimulated Microbubbles. Plos One. 2012; 7(12).
[4] Yan F, Li X, Jin Q, et al. Therapeutic Ultrasonic Microbubbles Carrying Paclitaxel and LyP-1 Peptide: Preparation, Characterization and Application to Ultrasound-Assisted Chemotherapy in Breast Cancer Cells. Ultrasound in Medicine & Biology. 2011; 37(5):768-79.
[5] Choijamts B, Naganuma Y, Nakajima K, et al. Metronomic irinotecan chemotherapy combined with ultrasound irradiation for a human uterine sarcoma xenograft. Cancer Science. 2011; 102(2):452-9.
[6] Nomikou N, Li YS, McHale AP. Ultrasound-enhanced drug dispersion through solid tumours and its possible role in aiding ultrasound-targeted cancer chemotherapy. Cancer Letters. 2010; 288(1):94-8.
[7] Hernot S, Klibanov A. Microbubbles in ultrasound-triggered drug and gene delivery ☆ . Advanced Drug Delivery Reviews. 2008; 60(10):1153-66.
[8] Lee J, Karshafian R, Papanicolau N, et al. QUANTITATIVE ULTRASOUND FOR THE MONITORING OF NOVEL MICROBUBBLE AND ULTRASOUND RADIOSENSITIZATION. Ultrasound in Medicine and Biology. 2012; 38(7):1212-21.
[9] Czarnota GJ, Karshafian R, Burns PN, et al. Tumor radiation response enhancement by acoustical stimulation of the vasculature. Proc Natl Acad Sci USA. 2012; 109(30):E2033-41.
[10] Todorova M, Agache V, Mortazavi O, et al. Antitumor effects of combining metronomic chemotherapy with the antivascular action of ultrasound stimulated microbubbles. International Journal of Cancer. 2013; 132(12):2956-66.
[11] Treat LH, McDannold N, Vykhodtseva N, et al. Targeted delivery of doxorubicin to the rat brain at therapeutic levels using MRI-guided focused ultrasound. Int J Cancer. 2007; 121(4):901-7.
[12] Zhao Y-Zea. Enhancing chemotherapeutic drug inhibition on tumor growth by ultrasound: an in vivo experiment. Journal of Drug Targeting. 2011; 19(2):154-60.
[13] Goertz DE, Karshafian R, Hynynen K. Antivascular effects of pulsed low intensity ultrasound and microbubbles in mouse tumors. Ultrasonics Symposium, 2008 IUS 2008 IEEE. 2008:670-3.
[14] Tarapacki C, Karshafian R. Enhancing laser therapy using PEGylated gold nanoparticles combined with ultrasound and microbubbles. Ultrasonics. 2015; 57:36-43.
[15] Tarapacki C, Kumaradas C, Karshafian R. Enhancing laser thermal-therapy using ultrasound-microbubbles and gold nanorods of in vitro cells. Ultrasonics. 2013; 53(3):793-8.
[16] Karshafian R, Bevan P, Williams R, et al. Sonoporation by Ultrasound-Activated Microbubble Contrast Agents: Effect of

Acoustic Exposure Parameters on Cell Membrane Permeability and Cell Viability. Ultrasound in medicine & biology. 2009; 35(5):847-60.
[17] Karshafian R, Samac S, Bevan P, et al. Microbubble mediated sonoporation of cells in suspension: Clonogenic viability and influence of molecular size on uptake. Ultrasonics. 2010.
[18] Chen W-S, Brayman AA, Matula TJ, et al. The pulse length-dependence of inertial cavitation dose and hemolysis. Ultrasound in medicine & biology. 2003; 29(5):739-48.
[19] Hu YX, Wan JMF, Yu ACH. Membrane Perforation and Recovery Dynamics in Microbubble-Mediated Sonoporation. Ultrasound in Medicine and Biology. 2013; 39(12):2393-405.
[20] Kumon R, Aehle M, Sabens D, et al. Spatiotemporal Effects of Sonoporation Measured by Real-Time Calcium Imaging. Ultrasound in medicine & biology. 2008:13.
[21] Deng CX, Sieling F, Pan H, et al. Ultrasound-induced cell membrane porosity. Ultrasound in medicine & biology. 2004; 30(4):519-26.
[22] Nofiele JIT, Karshafian R, Furukawa M, et al. Ultrasound-Activated Microbubble Cancer Therapy: Ceramide Production Leading to Enhanced Radiation Effect in vitro. Technology in Cancer Research & Treatment. 2013; 12(1):53-60.
[23] Al-Mahrouki AA, Karshafian R, Giles A, et al. Bioeffects of Ultrasound-Stimulated Microbubbles on Endothelial Cells: Gene Expression Changes Associated with Radiation Enhancement in Vitro. Ultrasound in Medicine and Biology. 2012; 38(11):1958-69.
[24] Kim HC, Al-Mahrouki A, Gorjizadeh A, et al. Quantitative Ultrasound Characterization of Tumor Cell Death: Ultrasound-Stimulated Microbubbles for Radiation Enhancement. Plos One. 2014; 9(7).
[25] Duvshani-Eshet M, Benny O, Morgenstern A. Therapeutic ultrasound facilitates antiangiogenic gene delivery and inhibits prostate tumor growth. Molecular Cancer Therapeutics. 2007.
[26] Wood AK, Ansaloni S, Ziemer LS, et al. The antivascular action of physiotherapy ultrasound on murine tumors. Ultrasound in medicine & biology. 2005; 31(10):1403-10.
[27] Hwang JH, Brayman AA, Reidy MA, et al. Vascular effects induced by combined 1-MHz ultrasound and microbubble contrast agent treatments in vivo. Ultrasound in medicine & biology. 2005; 31(4):553-64.
[28] Bing KF, Howles GP, Qi Y, et al. Blood-Brain Barrier (BBB) Disruption Using a Diagnostic Ultrasound Scanner and Definity® in Mice. Ultrasound in medicine & biology. 2009; 35(8):1298-308.
[29] Kong T, Zeng J, Wang XP, et al. Enhancement of radiation cytotoxicity in breast-cancer cells by localized attachment of gold nanoparticles. Small. 2008; 4(9):1537-43.
[30] Zhang XJ, Xing JZ, Chen J, et al. Enhanced radiation sensitivity in prostate cancer by gold-nanoparticles. Clinical and Investigative Medicine. 2008; 31(3):E160-E7.
[31] Pignol JP, Rakovitch E, Beachey D, et al. Clinical significance of atomic inner shell ionization (ISI) and Auger cascade for radiosensitization using IUdR, BUdR, platinum salts, or gadolinium porphyrin compounds. International Journal of Radiation Oncology Biology Physics. 2003; 55(4):1082-91.
[32] Hainfeld JF, Slatkin DN, Focella TM, et al. Gold nanoparticles: a new X-ray

contrast agent. British Journal of Radiology. 2006; 79(939):248-53.
[33] Popovtzer R, Agrawal A, Kotov NA, et al. Targeted Gold Nanoparticles Enable Molecular CT Imaging of Cancer. Nano Letters. 2008; 8(12):4593-6.
[34] Torchilin VP. Targeted pharmaceutical nanocarriers for cancer therapy and Imaging. Aaps Journal. 2007; 9(2):E128-E47.
[35] Hainfeld JF, Dilmanian FA, Slatkin DN, et al. Radiotherapy enhancement with gold nanoparticles. Journal of Pharmacy and Pharmacology. 2008; 60(8):977-85.
[36] Kennedy LC, Bear AS, Young JK, et al. T cells enhance gold nanoparticle delivery to tumors in vivo. Nanoscale Research Letters. 2011; 6.
[37] Chithrani BD, Ghazani AA, Chan WCW. Determining the size and shape dependence of gold nanoparticle uptake into mammalian cells. Nano Letters. 2006; 6(4):662-8.
[38] Trono JD, Mizuno K, Yusa N, et al. Size, Concentration and Incubation Time Dependence of Gold Nanoparticle Uptake into Pancreas Cancer Cells and its Future Application to X-ray Drug Delivery System. Journal of Radiation Research. 2011; 52(1):103-9.
[39] Chithrani DB, Dunne M, Stewart J, et al. Cellular uptake and transport of gold nanoparticles incorporated in a liposomal carrier'. Nanomedicine-Nanotechnology Biology and Medicine. 2010; 6(1):161-9.
[40] Pan Y, Neuss S, Leifert A, et al. Size-dependent cytotoxicity of gold nanoparticles. Small. 2007; 3(11):1941-9.
[41] Hauck TS, Ghazani AA, Chan WCW. Assessing the effect of surface chemistry on gold nanorod uptake, toxicity, and gene expression in mammalian cells. Small. 2008; 4(1):153-9.
[42] Chattopadhyay N, Cai ZL, Pignol JP, et al. Design and Characterization of HER-2-Targeted Gold Nanoparticles for Enhanced X-radiation Treatment of Locally Advanced Breast Cancer. Molecular Pharmaceutics. 2010; 7(6):2194-206.
[43] Bliss CI. The toxicity of poisons applied jointly. Annals of Applied Biology. 1939; 26(3):585-615.
[44] Lechtman E, Chattopadhyay N, Cai Z, et al. Implications on clinical scenario of gold nanoparticle radiosensitization in regards to photon energy, nanoparticle size, concentration and location. Physics in medicine and biology. 2011; 56(15):4631-47.
[45] Hao YZ, Yang XY, Song S, et al. Exploring the cell uptake mechanism of phospholipid and polyethylene glycol coated gold nanoparticles. Nanotechnology. 2012; 23(4).
[46] Kumar R, Roy I, Ohulchanskky TY, et al. In Vivo Biodistribution and Clearance Studies Using Multimodal Organically Modified Silica Nanoparticles. Acs Nano. 2010; 4(2):699-708.
[47] Wang C, Jiang Y, Li X, et al. Thioglucose-bound gold nanoparticles increase the radiosensitivity of a triple-negative breast cancer cell line (MDA-MB-231). Breast Cancer.
[48] Wang CH, Li XH, Wang Y, et al. Enhancement of radiation effect and increase of apoptosis in lung cancer cells by thio-glucose-bound gold nanoparticles at megavoltage radiation energies. Journal of Nanoparticle Research. 2013; 15(5).
[49] Zhang XD, Guo ML, Wu HY, et al. Irradiation stability and cytotoxicity of gold nanoparticles for radiotherapy. International Journal of Nanomedicine. 2009; 4:165-73.
[50] Feril LB, Tachibana K, Ikeda-Dantsuji Y, et al. Therapeutic potential of low-intensity ultrasound (part 2): biomolecular effects, sonotransfection,

and sonopermeabilization. Journal of Medical Ultrasonics. 2008; 35(4):161-7.
[51] Stieger SM, Caskey CF, Adamson RH, et al. Enhancement of vascular permeability with low-frequency contrast-enhanced ultrasound in the chorioallantoic membrane model. Radiology. 2007; 243(1):112-21.
[52] Schlicher RK, Radhakrishna H, Tolentino TP, et al. Mechanism of intracellular delivery by acoustic cavitation. Ultrasound in medicine & biology. 2006; 32(6):915-24.

List of figures: